

Figure 6 Radiation pattern of the antenna at 20.20 GHz

in the design is highly reliable having been well-verified by measured results from many other applications.

### 3. REFLECTOR PERFORMANCE

To demonstrate the intended application of the horn as a feed for a dual-reflector antenna, we use the shaped [6] 4.6-m diameter Cassegrain design shown in Figure 5 as a Ka-band earth-station antenna. In accordance with the horn design, the half-subtended angle to the subreflector is  $20^\circ$  and, for acceptable performance, we require the overall antenna system to satisfy the ITU-R S465.5 specifications for co- and cross-polar sidelobe levels. The horn is assumed to be fixed with the focus of the antenna 65-mm inside the horn, when measured from the aperture, corresponding to the phase centre of the horn for a  $\pm 20^\circ$  angular range.

The radiation pattern of the antenna is plotted in Figure 6 for 20.2 GHz and in Figure 7 for 30.0 GHz. It shows that the sidelobe level is compliant with the ITU-R S465.5 template. A summary of the performance of the antenna is given in Table 2. The full cross-polarization isolation is also given in the table. This isolation is the difference between the on-axis level and the maximum level of cross-polarization of the antenna in the  $45^\circ$ -plane. In practice, an isolation of better than 30 dB within the  $-1$  dB contour region is required in the transmit band and the results in Table 2 show that such a requirement would be met by this antenna.

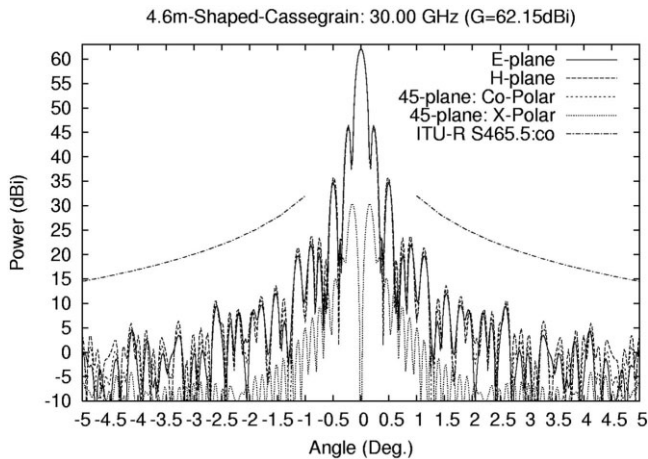


Figure 7 Radiation pattern of the antenna at 30.00 GHz

TABLE II  
Performance of the Antenna

Frequency (GHz)	Gain (Efficiency)	Xpol-Isolation
19.20	57.93 dBi (72.5%)	25.8dB
20.20	58.43 dBi (73.4%)	25.8dB
21.20	58.91 dBi (74.5%)	28.0dB
29.00	61.77 dBi (76.9%)	30.7dB
30.00	62.15 dBi (78.4%)	31.8dB
31.00	62.54 dBi (80.4%)	33.9dB

### 4. CONCLUSION

An example of a smooth-walled spline-profile Ka-band feed horn covering both the full commercial and military bands has been designed. To demonstrate its application, the horn has been used to feed a 4.6-m diameter dual-reflector antenna. It is expected that such a horn could be tailored to meet the specifications of other dual-reflector earth station antennas.

### REFERENCES

1. A.J. Parfitt, K.J. Greene, S.G. Hay, A.R. Forsyth, C. Granet, and S.J. Barker, Upgrade of an existing earth station for commercial and military applications using a new Ka-band feed system, IEEE Antennas Propagation Symposium, June 2003, Columbus, OH, Vol. 2, pp. 373–376.
2. C. Granet, G.L. James, R. Bolton, and G. Mooney, A smooth-walled spline-profile horn as an alternative to the corrugated horn for wide band millimeter-wave applications, IEEE Trans Antennas Propag 52 (2004), 848–854.
3. C. Granet and G.L. James, Spline-profile smooth-walled C-band horn, IEEE Antennas Wireless Propag Lett 6 (2007), 415–418.
4. I. Jensen, An optimized stepped profiled horn with low cross-polarization for a 20/30 GHz DVB-RCS terminal, 18th International Conference on Applied Electromagnetics and Communications, ICECOM, 2005, 4 p.
5. I. Jensen and J.A. Aas, A metallized plastic feed horn with optimized smooth-walled profile and low cross polarization at 20/30 GHz, Proceedings of the European Conference on Antennas and Propagation, EuCAP'07, Edinburgh, UK, Nov 11–16, 2007, 5 p.
6. G.L. James, Radiation pattern control of Cassegrain antennas, IEE Proc 134 (1987), 217–222.

© 2008 Wiley Periodicals, Inc.

## EXTREME PERFORMANCE TEM HORN

J. A. G Malherbe

Department of Electrical, Electronic, and Computer Engineering, University of Pretoria, Pretoria, South Africa 0002; Corresponding author: jagm@up.ac.za

Received 4 December 2007

**ABSTRACT:** Previously, a TEM horn with ultra wideband performance had been described. The horn made use of an elliptic plate separation profile, while the plate width was determined by an optimal impedance function and the characteristic impedance equations for microstrip. In this article, it is shown that if the impedance equations for parallel plate waveguide are employed in the calculation of the plate width, extreme bandwidth of more than 70:1 for a VSWR of 2:1 can be achieved. © 2008 Wiley Periodicals, Inc. Microwave Opt Technol Lett 50: 2121–2125, 2008; Published online in Wiley InterScience (www.interscience.wiley.com). DOI 10.1002/mop.23550

**Key words:** extreme bandwidth; TEM horn; elliptic profile

## 1. INTRODUCTION

The conventional approach to TEM horn design, is to consider the horn as a transition from a bound TEM line to free space. A variety of impedance matching networks, such as exponential [1], or the near optimal Hecken taper [2, 3] have been employed to obtain a wideband impedance match. The design principle is that of an impedance match between the feed line (typically  $50 \Omega$ ) and free space ( $120 \pi \Omega$ ). The variation of impedance obtained from the taper design is translated to dimensions using a preferred model for the radial line that constitutes the horn. The tapered TEM line is modeled variously as a microstrip line [3, 4] or as a parallel plate waveguide [1].

It was shown in [5] that a TEM horn can exhibit superior performance if the horn plate separation is an elliptic cross section, combined with a Hecken impedance taper and microstrip dimensions. In that case, a 15:1 bandwidth ratio had been achieved.

The essential mechanism of operation of the horn was investigated in [6]. It was postulated that the mechanism of radiation could be divided into three distinct regions, viz, the dipole region at the low frequency end, the “transformer” region where the modes are still bound to the entire length of the horn, and the horn region, where the radiation becomes increasingly detached from the outer end of the horn surface as the frequency increases. Bearing this in mind, it was shown that by judicious modification of the profile, a substantial improvement in bandwidth could be achieved. In that case, the bandwidth had increased to a ratio of 19:1 for a VSWR of 2.

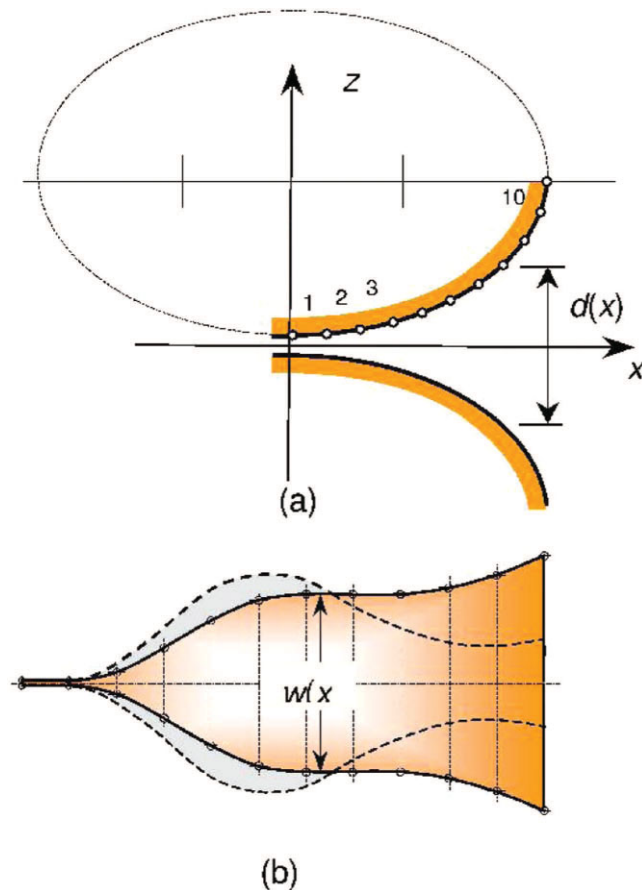


**Figure 1** (a) Profile of the elliptic horn, side view; (b) plate profile with parallel plate impedance equation compared to stripline equation (dashed line). [Color figure can be viewed in the online issue, which is available at [www.interscience.wiley.com](http://www.interscience.wiley.com)]

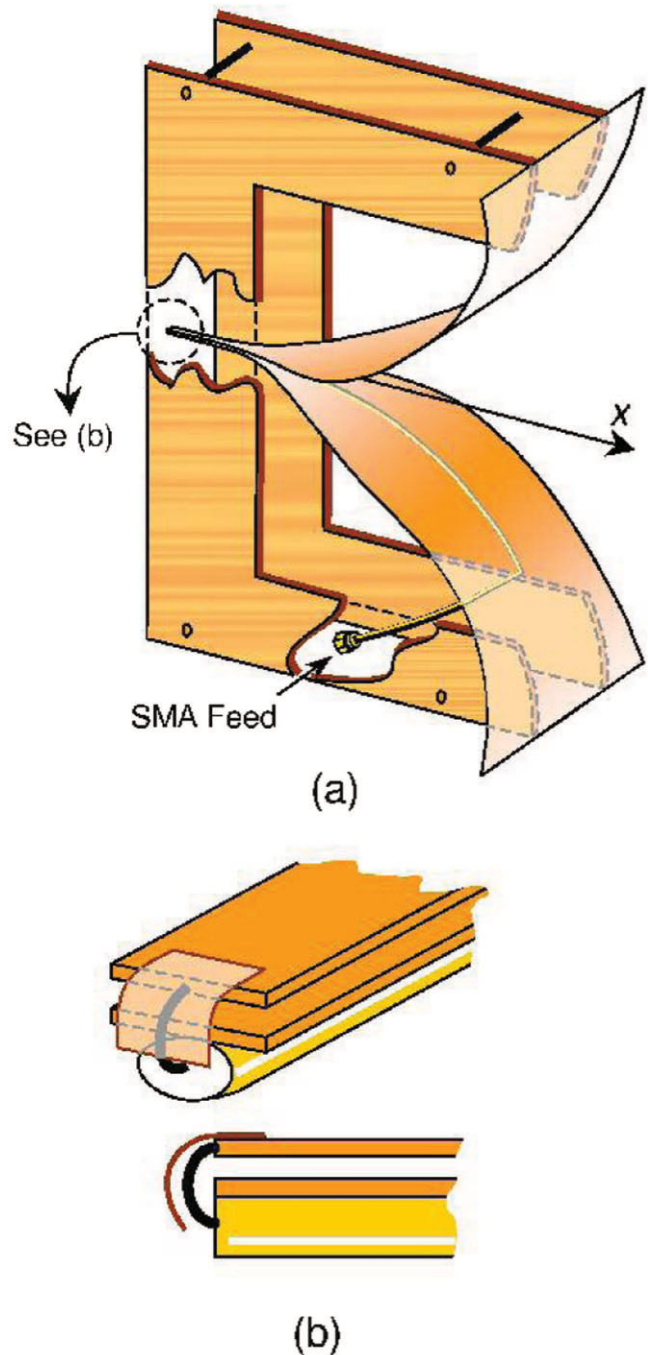


**Figure 2** Perspective view (a), showing the apex (b). [Color figure can be viewed in the online issue, which is available at [www.interscience.wiley.com](http://www.interscience.wiley.com)]

Subsequently, other profiles, based on a more analytical approach, were investigated, and it was found that a dramatic improvement in bandwidth resulted. The design and performance of such an extreme bandwidth TEM horn is described in this article.

## 2. HORN PROFILE

The horn profile employed is based on the elliptic separation function described in [5], and employs the same Hecken impedance function; the design, up to the point of realizing the horn dimensions, exactly follows that described in [5], and is not repeated here. The elliptical profile is shown in Figure 1(a). How-

**TABLE I Impedance and Line Dimensions for Taper**

$N-1$	0	1	2	3	4	5	6	7	8	9	10
$x$ [mm]	0.0	66.5	132.2	196.6	258.2	316.1	368.7	413.7	449.3	472.0	480.0
$Z_0(x)$ [ $\Omega$ ]	50.0	51.5	56.8	69.5	94.4	137.3	199.7	271.4	331.7	365.3	377.0
$d(x)$ [mm]	2.0	9.1	30.3	66.2	116.9	183.2	265.4	362.8	476.3	600.9	733.4
$w(x)$ [5]	12.1	52.9	156.8	266.2	313.4	285.3	215.4	154.6	121.0	114.4	127.2
$w(x)$ [mm]	7.5	32.9	100.8	176.4	234.1	251.5	250.7	252.5	270.8	309.9	367.0

ever, the plate width is calculated by means of the equations for parallel plate waveguide, as proposed in [1],

$$w(x) = \frac{120\pi}{Z_0(x)}d(x)$$

where  $Z_0(x)$  is the calculated horn impedance obtained from the impedance function,  $d(x)$  is the plate separation (elliptic profile), and  $w(x)$  the calculated plate width. As in [5] there are 10 sections of equal length of 66.48 mm, and the plate profile before being bent to the elliptic form is shown in Figure 1(b); the profile of the horn of [5] is shown in dashed lines and it is clear that the difference in shape between the two horns is quite dramatic.

### 3. CONSTRUCTION

Figure 2(a) shows the assembled horn. It is constructed from 0.5-mm brass plate, formed over a wooden mandrill to obtain the elliptic shape. Two plywood sections maintain rigidity of the structure, and are affixed to the outside of the horn flare by means of countersunk screws. The horn is fed at its apex by means of a semi-rigid coaxial line, which is run along the outer surface of the lower horn plate. Where the coaxial feed line terminates at the apex of the lower plate, the centre conductor of the coaxial line is exposed, and folded over and soldered to the end of the other (upper) plate. From this plate, a thin metal foil tab runs back over the folded centre conductor as shown in Figure 2(b); this tab is adjusted to compensate for the stray reactances in the feed point region.

The connector feed end of the coaxial feed line is affixed to the horn in an area of minimum surface current, and thus very little unbalanced earth current flows to the horn, as described in [7], obviating the need for a discrete balun.

Table 1 shows the horn impedance,  $Z_0(x)$ , and dimensions  $d(x)$  and  $w(x)$ , as a function of distance  $x$  along the length of the horn; the width  $w(x)$  for the horn in [5] is also included.

### 4. PERFORMANCE

Figure 3(a) shows the expanded response of VSWR versus frequency for the low frequency region, while Figure 3(b) shows the VSWR to 18 GHz. To all intents and purposes, the VSWR lies below 2 from 250 MHz to 17.5 GHz, or a bandwidth ratio of 70:1. The horn is fed by a length of  $\sim 1.2$  m of cable, and the cable loss was factored into the VSWR responses shown in Figure 3.

$E$ - and  $H$ -plane radiation patterns were measured and calculated for a number of different frequencies, and are shown in Figures 4(a)–4(f), for frequencies of 500 MHz, and 4 and 12 GHz, for both  $E$  and  $H$  plane polarization. Measured sidelobe levels remain nominally below  $-10$  dB at all frequencies.

Figure 5 shows calculated and measured gain responses. As with the return loss, the gain was compensated for the feed cable.

The horn was analyzed by means of the commercial software FEKO<sup>®</sup>, and the calculated performance is shown in each

instance as a dotted line. The horn is, apart from its physical size, electrically extremely large at the upper frequency end; the plate length along the surface is some 665 mm, and the width is 367 mm at the aperture, which stands 733-mm high. In order for the numerical analysis to retain its accuracy, the moment method mesh used was  $\lambda/9$ .

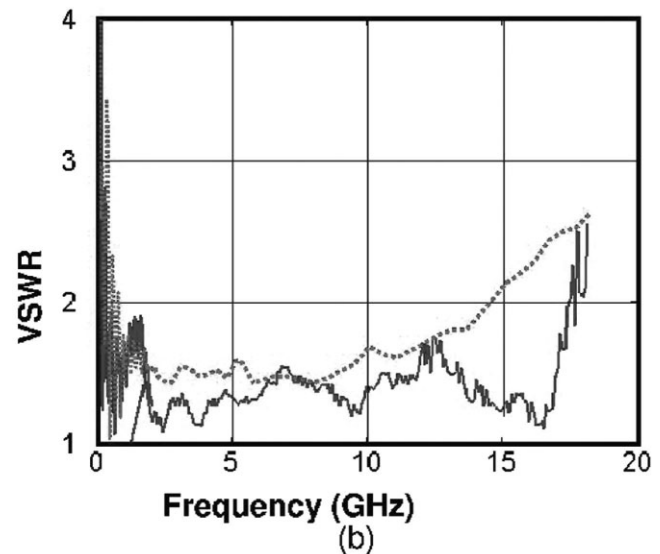
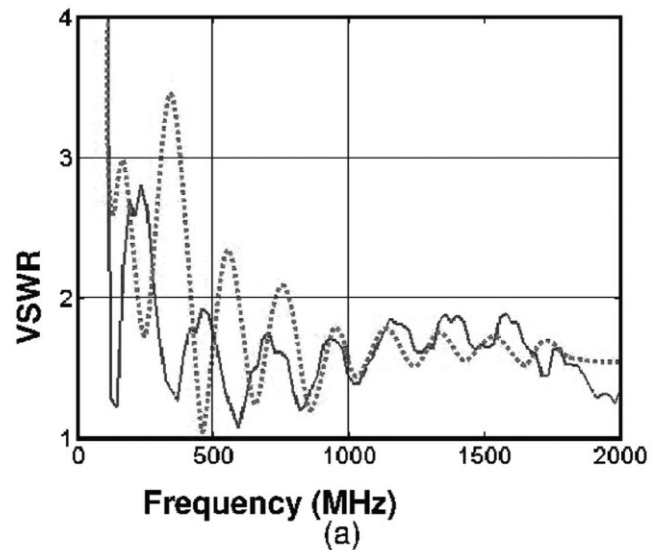


**Figure 3** Response of VSWR versus frequency. (a) Expanded lower frequency region, and (b) VSWR through 18 GHz. — Measured . . . . . Calculated. [Color figure can be viewed in the online issue, which is available at [www.interscience.wiley.com](http://www.interscience.wiley.com)]

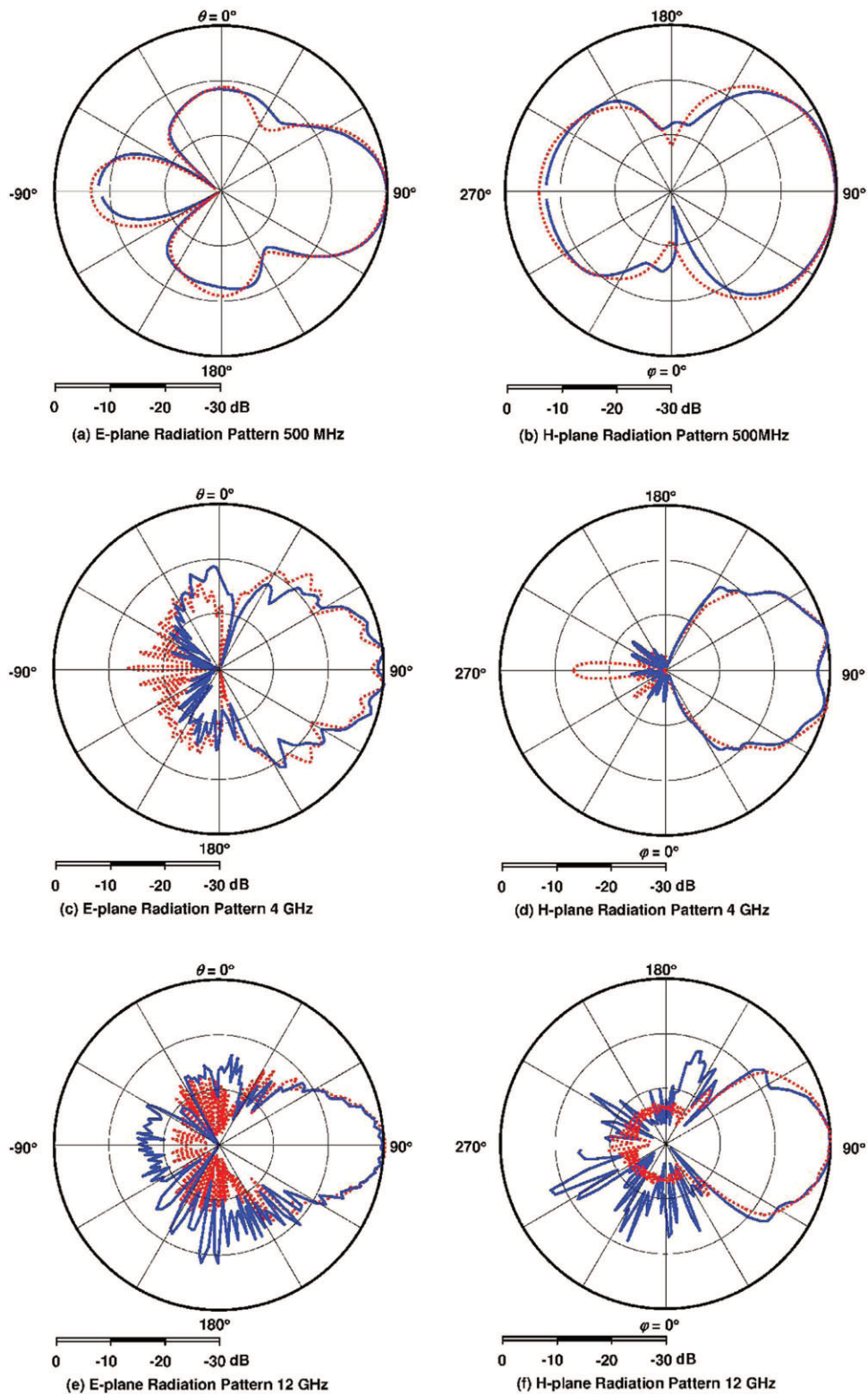


**Figure 4** *E* and *H* plane radiation patterns. (a) and (b): 500 MHz; (c) and (d): 4 GHz; (e) and (f): 12 GHz. \_\_\_\_ Measured . . . . . Calculated. [Color figure can be viewed in the online issue, which is available at [www.interscience.wiley.com](http://www.interscience.wiley.com)]

## 5. DISCUSSION

In Figure 3 it can be seen that the measured and calculated VSWR track accurately to 2 GHz, and that good correspondence is noted at the higher frequencies. The disparity between calculated and measured gain increases with frequency (see Fig. 5). The radiation

patterns correspond extremely well, the only substantial difference being in the sidelobe level at the higher frequency.

The large drop in gain between 11 and 12 GHz is caused by the stimulation of higher order modes in the throat of the horn, which is not predicted by the ideal numerical calculation. Bearing in mind

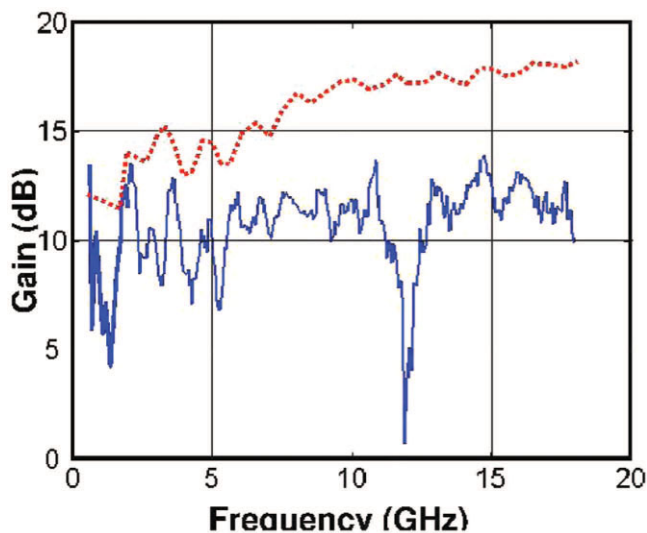


**Figure 5** Response of Gain versus frequency. \_\_\_\_ Measured ..... Calculated. [Color figure can be viewed in the online issue, which is available at [www.interscience.wiley.com](http://www.interscience.wiley.com)]

that the construction of the horn is far from ideal, the deviations from the predicted values are to be expected. While the width curvature of the horn is easy to manufacture, obtaining the precise separation curvature and maintaining the correct plate separation is problematic. This would account for the deviations seen in VSWR and sidelobes at the higher frequencies.

## 6. CONCLUSION

The performance of an extreme bandwidth horn has been described. By making use of the parallel plate waveguide equations to model the characteristic impedance of a radial line, and combined with an elliptic plate separation and Hecken near optimal impedance function, a “TEM” horn of extreme bandwidth was designed. The VSWR remains below 2 from 250 MHz to 17.5 GHz, and the radiation pattern is stable, with sidelobes generally below  $-10$  dB.

Because of the thin metal gauge, it is virtually impossible to construct the area around the apex accurately, and a profile machined from much thicker and inherently stable material would exhibit a much more uniform gain response. It is also expected that the deep dip in gain, most probably caused by a higher order mode being generated, would be evened out.

## ACKNOWLEDGMENT

The author wishes to express his appreciation to the staff of FEKO who provided extensive support and performed the high frequency calculations, Lukas Naudé for performing the measurements, and Johan Joubert for many valuable discussions.

## REFERENCES

1. H. Choi and S. Lee, Design of an exponentially-tapered TEM horn antenna for the wide broadband communication, *Microwave Opt Technol Lett* 40 (2004), 531–534.
2. K.L. Shlager, G.S. Smith, and J.G. Maloney, Accurate analysis of TEM horn antennas for pulse radiation, *IEEE Trans Electromagn Compat* 38 (1996), 414–423.
3. Y. Huang, M. Nakhkash, and J.T. Zhang, A dielectric material loaded TEM horn antenna, *ICAP 2003, 12th Intl Conf. Ant. Prop., ICAP 2003, (Conf. Publ. No. 491) Vol. 2, 31 March–3 April 2003, pp. 489–492.*
4. A.S. Turk, Ultra-wideband TEM horn design for ground penetrating

- impulse radar systems, *Microwave Opt Technol Lett* 41 (2004), 333–336.
5. J.A.G. Malherbe and N.S. Barnes, TEM horn antenna with an elliptic profile, *Microwave Opt Technol Lett* 49 (2007), 1548–1551.
6. J.A.G. Malherbe, Design of ultra wideband TEM horns, to be presented at 2007 Asia Pacific Microwave Conference, APMC 2007, Bangkok, Thailand, Dec. 2007.
7. M. Manteghi and Y. Rahmat-Samii, A novel UWB feeding mechanism for the TEM horn antenna, reflector IRA, and the Vivaldi antenna, *IEEE Antennas Propagat Mag* 46 (2004), 81–87.
8. FEKO©; EM Software and Systems-S.A. (Pty) Ltd. Available at: <http://www.feko.info/index.html>.

© 2008 Wiley Periodicals, Inc.

## DUAL-FREQUENCY CIRCULARLY-POLARIZED MICROSTRIP ANTENNA WITH SWITCHABLE POLARIZATION SENSE

Jia-Feng Wu,<sup>1</sup> Jeen-Sheen Row,<sup>1</sup> and Kin-Lu Wong<sup>2</sup>

<sup>1</sup> Department of Electrical Engineering National Changhua University of Education Chang-Hua, Taiwan 500, Republic of China; Corresponding author: [isrow@cc.ncue.edu.tw](mailto:isrow@cc.ncue.edu.tw)

<sup>2</sup> Department of Electrical Engineering National Sun Yat-Sen University Kaohsiung, Taiwan 804, Republic of China

Received 6 December 2007

**ABSTRACT:** A dual-frequency circularly-polarized (CP) microstrip antenna capable of switching polarization sense is presented. The antenna is fed by a microstrip line through aperture coupling. First, it is found that a CP mode can be excited when the radiating patch is square and an open-ring slot is used as the coupling aperture. Then, by truncating the radiating patch, another CP mode can be obtained. The two CP modes have reversed polarization senses, and their operating frequencies are different. For the proposed dual-frequency CP microstrip antenna, two prototypes with frequency ratios of 1.07 and 1.23 were constructed, and voltage-controlled diodes are employed to achieve the electrical switching between the two CP modes. © 2008 Wiley Periodicals, Inc. *Microwave Opt Technol Lett* 50: 2125–2128, 2008; Published online in Wiley InterScience ([www.interscience.wiley.com](http://www.interscience.wiley.com)). DOI 10.1002/mop.23569

**Key words:** microstrip antenna; dual-frequency operation; switchable polarization

## 1. INTRODUCTION

It is well-known that circular polarization (CP) radiations can be produced from a linearly-polarized (LP) microstrip antenna by the method of truncating patch corners, and the polarization sense of the obtained CP is determined by the position of the truncated corners. On the basis of the method, several designs for the microstrip antenna with the polarization switching between LP and CP or between right-hand circular polarization (RHCP) and left-hand circular polarization (LHCP) have been presented [1–3]. For these reported designs, PIN diodes or other electrical devices are used to reconfigure the truncated corners, and the antennas are operated at the same frequency while the polarization is switched. To simultaneously obtain frequency diversity, a U-shaped slot is embedded to the radiating patch with the reconfigurable truncated corners, and the antenna can provide CP and LP radiations at two different frequencies [4]. In addition, by cutting a reconfigurable thin slot in a nearly square patch, the microstrip antenna that is